

Article

Biodiesel from Waste Cooking Oil: Highly Efficient Homogeneous Iron(III) Molecular Catalysts

Vincenzo Langelotti ^{1,†}, Massimo Melchiorre ^{1,2,†}, Maria Elena Cucciolito ^{1,3}, Roberto Esposito ^{1,3},
Domenico Grieco ¹, Gabriella Pinto ¹ and Francesco Ruffo ^{1,3,*}

¹ Department of Chemical Sciences, University of Naples Federico II, University Campus of Monte S. Angelo, Via Cintia 21, 80126 Naples, Italy; vincenzo.langellotti@unina.it (V.L.); massimo.melchiorre@unina.it (M.M.); cuccioli@unina.it (M.E.C.); roberto.esposito@unina.it (R.E.); domenico6022@gmail.com (D.G.); gabriella.pinto@unina.it (G.P.)

² ISUSCHEM srl, Piazza Carità 32, 80134 Naples, Italy

³ Interuniversity Consortium of Chemical Reactivity and Catalysis (CIRCC), Via Celso Ulpiani 27, 70126 Bari, Italy

* Correspondence: ruffo@unina.it

† These authors contributed equally to this work.

Abstract: This article presents an efficient iron(III) molecular catalyst for the production of biodiesel from waste vegetable oils. The approach involved an initial screening of eight salophen complexes with various substituents on the arene rings, leading to the selection of the simplest unsubstituted species as the most active catalyst. Under optimized conditions, this catalyst demonstrated the capability to achieve complete conversion of the oil at a low catalyst loading (0.10% mol/mol) and convenient conditions (160 °C, 20/1 MeOH/oil ratio).

Keywords: iron(III); salophen; homogeneous catalysis; transesterification; waste vegetable oil



Citation: Langelotti, V.; Melchiorre, M.; Cucciolito, M.E.; Esposito, R.; Grieco, D.; Pinto, G.; Ruffo, F. Biodiesel from Waste Cooking Oil: Highly Efficient Homogeneous Iron(III) Molecular Catalysts. *Catalysts* **2023**, *13*, 1496. <https://doi.org/10.3390/catal13121496>

Academic Editor: Claudia Carlucci

Received: 29 October 2023

Revised: 1 December 2023

Accepted: 5 December 2023

Published: 7 December 2023



Copyright: © 2023 by the authors. Licensee MDPI, Basel, Switzerland. This article is an open access article distributed under the terms and conditions of the Creative Commons Attribution (CC BY) license (<https://creativecommons.org/licenses/by/4.0/>).

1. Introduction

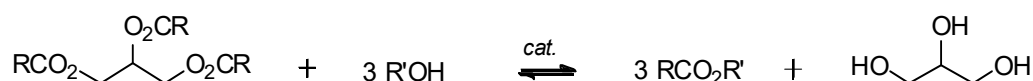
A modern biorefinery is a facility that integrates processes of biomass conversion to produce a spectrum of bio-based products (including food, animal feed, chemicals, and materials) and bioenergy (comprising biofuels, energy, and/or heat). Initially, the concept of biorefinery was primarily focused on energy production (first-generation biorefinery). Second-generation biorefinery aimed to produce both energy and chemicals from conventional food crops such as corn, wheat, palm, and rapeseed. However, this choice raised numerous ethical concerns as it involved using food crops, diverting them from their primary use. For this reason, the concept of third-generation biorefinery has gained prominence in recent years. Third-generation biorefineries implement the conversion of residual or waste crops that do not compete with the food chain. Even more rigorously, these facilities advocate the utilization of local resources and therefore feedstock aligned with the natural productive features of the region in which they are installed [1,2]. The generation of electricity can serve for self-use and possible sale to the local community. High-value products increase profitability, fuel helps meet energy needs, and electricity production contributes to reducing energy costs and greenhouse gas emissions.

The research presented here aims to contribute to the growth of this industrial model by combining the versatility of residual biomass with the principles of Green Chemistry, which plays a significant role in modern synthetic chemistry. This includes considerations such as a low E-factor, a high atom economy, minimal use of solvents, and the adoption of catalytic methods [3].

In this context, biodiesel is well-acknowledged as an advantageous alternative fuel compared to diesel derived from fossil sources [4]. In addition to its renewable origin, other benefits are evident: it is carbon neutral, meaning its combustion does not produce

additional carbon dioxide; it is biodegradable due to the presence of oxygenated linear carbon atom chains (in contrast to fossil diesel, which contains numerous long chains devoid of oxygen, as well as cyclic aliphatic hydrocarbons and polycyclic aromatic hydrocarbons). Biodiesel does not contain harmful metal ions of cadmium, lead, and vanadium, nor organic aromatic compounds that are harmful to humans, while containing only trace amounts of sulfur (<0.001%) [5]. Finally, it has a higher flash point (100–150 °C) compared to fossil diesel (≈ 40 °C), so it is not classified as a hazardous material and is safer to handle and store [6].

Biodiesel is produced by transesterification of the triglycerides present in vegetable oils with light alcohols, typically methanol ($R' = \text{Me}$), according to Scheme 1.



Scheme 1. Transesterification of triglycerides to produce biodiesel and glycerol.

The product is a mixture of fatty acid methyl esters (FAME's or biodiesel) and glycerol. The latter, which represents about 10% by mass of the produced biodiesel, is one of the most interesting chemical platforms for preparing bio-based products today [7].

As mentioned before, in compliance with the principles of circular and green economies, the vegetable feedstock must not compete with the chain food. Therefore, it preferably derives from marginal crops or waste of the agro-food industry. In this context, exhausted cooking oils play an important role [8,9], because their recovery from catering or domestic consumption is assuming increasing dimensions. In Italy, the total amount of oil collected in 2018 has reached around 76,000 tons out of the 260,000 produced, in a constant positive trend [10].

There are drawbacks associated with the processing of these raw materials. First, the transesterification of Scheme 1 is an equilibrium, which must be shifted towards the products to have acceptable yields. This is typically achieved by using an excess of methanol. Second, the reaction must be catalyzed to ensure adequate production rates. Although Brønsted's bases have undeniable good performance [11], their use is compromised or complicated by the presence of free fatty acids [12], whose concentration increases upon cooking [13]. For this reason, Lewis acid catalysts based on cheap metals have been proposed as an alternative, both homogeneous (e.g., complexes of Zn(II) [14–17], Sn(IV) [18,19] or Fe(III) [20]) or heterogeneous (metal oxides [21–24], their mixtures or salts) that simultaneously promote transesterification of triglycerides (Scheme 1) and esterification of free fatty acids (Scheme 2).



Scheme 2. Esterification of fatty acids to produce biodiesel.

Pros of the former catalysts are high activity and tailored structure design, while their cons are the difficult separation from the products and recycling. On the other hand, heterogeneous catalysts are often less performing, also due to the establishment of internal mass transfer equilibria which could depress the yield [25]. However, recycling is easier as long as there is no leaching of the metal ions in the product phase.

Recently, we proposed salen iron(III) complexes (**1** in Figure 1) as homogeneous catalysts for the production of biodiesel [20].

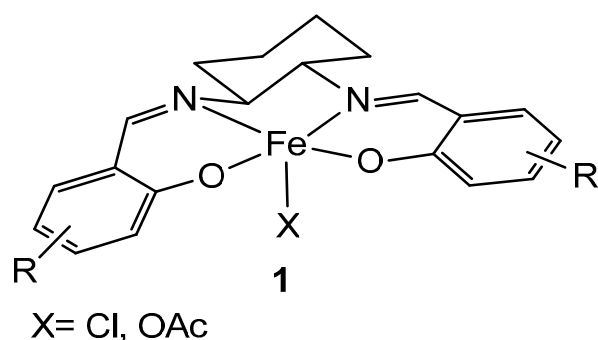
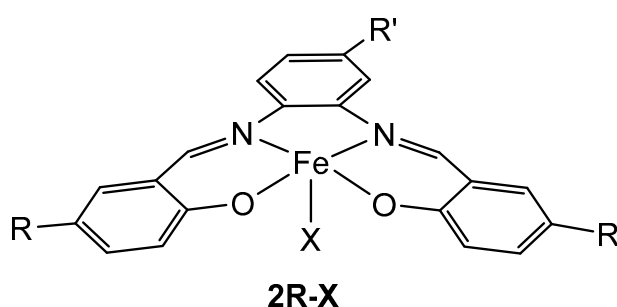


Figure 1. General structure of salen complexes of type 1.

At low iron loadings (0.1% mol(Fe)/mol(oil)), a 90% conversion of a waste cooking oil (WCO) was achieved in convenient conditions, and the percentage of iron found in biodiesel was in many cases a few ppm. Motivated to further improve the performance of the catalysts, we redesigned their structure by replacing the cyclohexanediamine portion with *o*-phenylenediamine, aiming to preserve the catalytic activity while reducing steric hindrance. The option of also functionalizing the aromatic ring of the ligand backbone (known as salophen) was also taken into account. Given this premise, eight complexes of iron(III)-containing salophen ligands were prepared and used in the production of biodiesel from vegetable oils (Figure 2).



2H-OAc: R= H, R'=H, X= OAc

2Me-OAc: R= Me, R'=H, X= OAc

2OMe-OAc: R= OMe, R'=H, X= OAc

2H-Cl: R= H, R'=H, X= Cl

2Me-Cl: R= Me, R'=H, X= Cl

2OMe-Cl: R= OMe, R'=H, X= Cl

2'H-OAc: R= H, R'= NO₂; X= OAc

2''H-OAc: R= H, R'= NH₂; X= OAc

Figure 2. Structure of salophen-based catalysts.

The extensive availability of substituted hydroxybenzaldehydes, which are essential precursors for ligand preparation, allowed full exploitation of the versatility of homogeneous catalysis, which is based on the tailored and accurate selection of the coordination environment of the active metal ion. It is also important to emphasize that similar compounds have recently received attention for their role as Lewis acid catalysts in reactions involving the cyclization of CO₂ for cyclic carbonate formation and the polymerization of lactide [26].

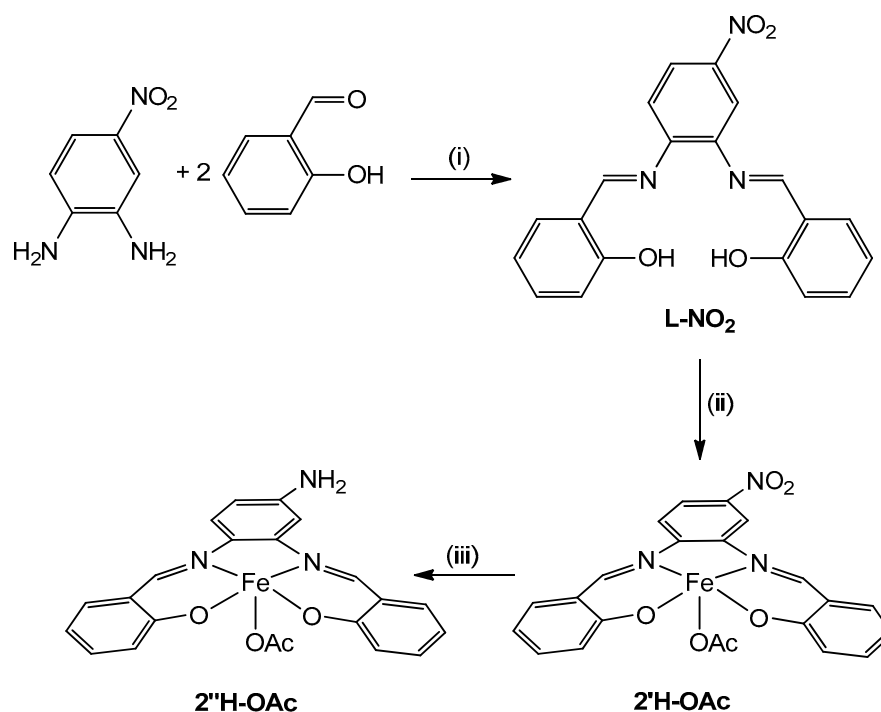
In this work, we demonstrate that our approach also proved to be successful. In fact, an initial screening of all the complexes allowed identification of **2H-OAc** as the most active one, a circumstance that is particularly favorable since it is the most cost effective and straightforward to synthesize. Subsequently, the same catalyst was employed in the transesterification of an authentic waste cooking oil, and, under optimized conditions, it promoted its complete conversion to biodiesel.

2. Results and Discussion

Biodiesel Synthesis with Salophen Complexes

Eight homogeneous catalysts were selected for an initial screening (Figure 2). Six of them have different substituents on the salophen ligand (H, Me or OMe), and vary in the nature of the fifth anionic ligand that can be acetate or chloride. Other less coordinating anions (e.g., triflate, trifluoroacetate, tetrafluoroborate) were not considered since they have already returned less satisfactory results in a previous investigation [20]. Catalysts **2H-OAc**, **2H-Cl** and **2OMe-Cl** are described in the literature [26–28], while the other three unpublished complexes, **2Me-OAc**, **2Me-Cl** and **2OMe-OAc**, were analogously prepared by reacting iron(II) acetate or iron(III) chloride with the appropriate salophen ligand under air (synthesis details in the experimental section; melting points and FT-IR spectra are collected in the supporting materials, Figures S1–S5 and Table S1).

The remaining two complexes differ in the presence of a substituent in the arene ring of the backbone, either electron withdrawing (**2'H-OAc**) or electron donor (**2''H-OAc**). Their complete preparation is shown in Scheme 3.



(i) toluene, Δ ; (ii) $\text{Fe}(\text{OAc})_2$, air, ethanol, Δ ; (iii) bis(pinacolato)diboron, *t*-BuOK, *i*-propanol, Δ

Scheme 3. Synthetic strategy for catalysts **2'H-OAc** and **2''H-OAc**.

The first step is the synthesis of ligand **L-NO₂**. Surprisingly, although described in the literature, none of the proposed syntheses [29] satisfactorily yielded the desired product. Very often, a mixture of mono- and di-substituted species was isolated at the end of the reactions, and in many cases, neither extending the reaction times nor refluxing in ethanol was revealed to be helpful. It is probable that the presence of the nitro group inhibits reactivity in the condensation reaction, and it was, therefore, possible to isolate the product **L-NO₂** in high yields only after 20 h of reflux in toluene in the presence of a large excess of salicylaldehyde (details in experimental section). The proton NMR spectrum of the ligand is shown in Figure 3, where the two non-equivalent halves of the ligand can be appreciated, particularly the two –OH protons at δ 12.54 and 12.47, and the two imine protons at δ 8.73 and 8.65.

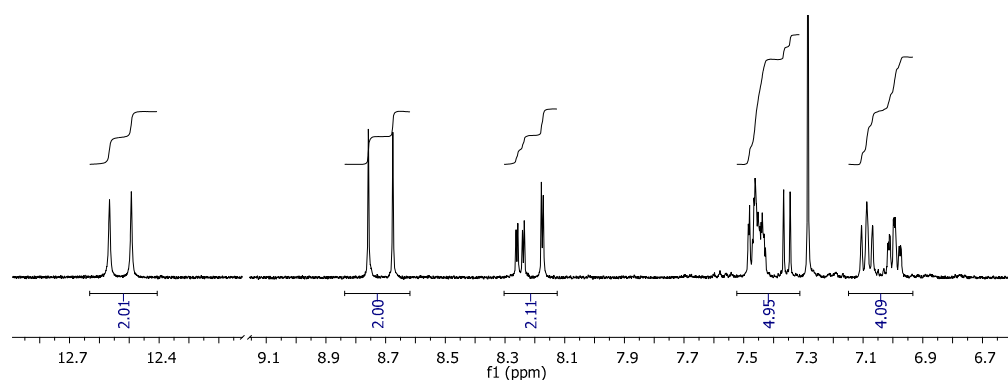


Figure 3. Significant portions of the ^1H NMR spectrum of L-NO_2 recorded at 500 MHz at 298 K in CDCl_3 .

Coordination of L-NO_2 to the iron(III) ion was carried out as for the other catalysts, by refluxing a mixture of iron(II) acetate and the ligand in ethanol. The reddish complex $2'\text{H-OAc}$ was then treated with the reducing agent bis(pinacolato)diboron in basic *i*-propanol to reduce the nitro group to amine [30], and the corresponding catalyst $2''\text{H-OAc}$ was isolated after 24 h of reaction.

Mass and IR spectra did confirm the identity of all the complexes. In particular, the IR spectra stacks of 2H-OAc , $2'\text{H-OAc}$ and $2''\text{H-OAc}$ are reported in Figure 4. The spectrum of $2'\text{H-OAc}$ showed the presence of two bands at 1575 (s) and 1343 (s) cm^{-1} relating to the symmetrical and asymmetrical stretching of the NO_2 group. These were no longer present in the spectrum of $2''\text{H-OAc}$, while the broad band of the amino group appeared around 3347 (w, br) cm^{-1} .

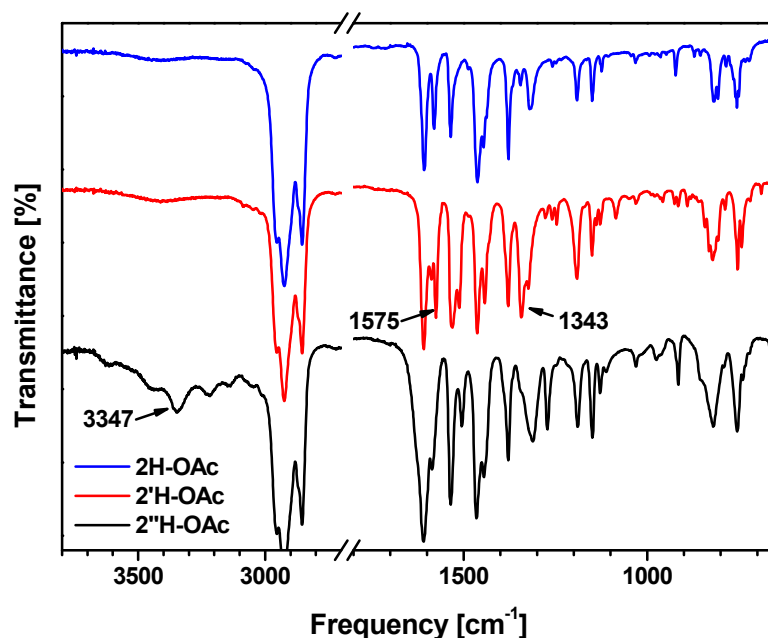


Figure 4. 2H-OAc , $2'\text{H-OAc}$ and $2''\text{H-OAc}$ relevant portion of FT-IR spectra. Nujol related peaks at 2900 (sat), 1461 (s), 1376 (s), 721 (m) cm^{-1} .

Biodiesel production was performed under continuous stirring in a batch Parr[®] stainless steel reactor, equipped with a thermostatic heating band. Early experiments were carried out with fresh commercial soybean oil (see Footnote b of Table 1 for the oil properties) at a temperature of 160 °C, with a catalyst loading of 0.10% mol(Fe)/mol(oil) and a 10/1 methanol/oil molar ratio. After reaction quenching, methanol was evaporated,

and the resulting mixture was analyzed by $^1\text{H-NMR}$ spectroscopy to evaluate the yield (Table 1).

Table 1. Biodiesel yields ^a using the set of catalysts on fresh soybean oil ^b.

Entry	Catalyst	Yield, %
1	2H-OAc	87 ± 2
2	2H-Cl	86 ± 2
3	2Me-OAc	85 ± 2
4	2Me-Cl	84 ± 2
5	2OMe-OAc	83 ± 2
6	2OMe-Cl	82 ± 2
7	2'H-OAc	66 ± 2
8	2''H-OAc	67 ± 2

^a T = 160 °C; t = 2 h; mol(Fe)/mol(oil) = 0.001/1; mol(MeOH)/mol(oil) = 10/1. ^b AV = 0.10 mg(KOH)/g(oil); peroxide value = 2.0 meq(O₂)/kg(oil); iodine value: 129 g(I₂)/100 g(oil). Soybean fatty acid composition: SFAs 14%_{mol}, MUFAs 27%_{mol}, PUFAs 59%_{mol}.

The screening allowed comparison of some key structural aspects of the catalysts, such as the nature of the fifth ligand on the iron ion, and the effect of the substituents both on the external aromatic rings and on the arene backbone. It is interesting to note that the trend reveals that donor substituents on the outer rings make the catalytic species less active, according to the OMe < Me < H trend, both in complexes with acetate (Entries 5, 3 and 1) and complexes with chloride (Entries 6, 4 and 2) in the fifth coordination position. This trend suggests that in some way, an increase in electron density on the metal reduces its Lewis acidity and therefore its performance. The comparison between complexes with chloride and those with acetate shows that the latter have higher catalytic activity. One possible explanation was provided in a previous study [20], in which the involvement of the acetate group in the activation of the carbonyl substrate was hypothesized. Another possible effect could be the greater coordinating ability of the chloride ligand compared to acetate, which partially inhibits the activity of the iron(III) ion, as the fifth coordination position is less available for the substrate.

On the other hand, it is remarkable to observe that two very different groups, such as nitro and amino placed on the backbone of the ligand, have the effect of inhibiting catalytic activity (Entries 7 and 8), even though one is a strong electron-withdrawing group and the other is an electron-donating group. In these cases, it can be observed that substitution on the central ring has a pronounced effect, and it draws attention to the fact that also an excessive reduction in the iron electron density, caused by the nitro group, can have a detrimental effect on catalytic activity. This can be justified by considering other studies, including pioneering ones by Tomita and Ida [31], who demonstrated that excessive Lewis acidity can inhibit the catalytic cycle by stabilizing inactive coordination compounds that contain the reaction product.

It emerges that the simplest catalyst, **2H-OAc**, shows the best performing electronic balance and therefore represents the best option. This is remarkably appreciable because it is the most economically and synthetically convenient.

Further tests were therefore performed using **2H-OAc** on waste sunflower oil (see Footnote b of Table 2 for oil properties). Real feedstocks are more complex matrices than fresh oils because they contain oxidation and decomposition products, as well as pollutants from thermal treatment of food residues. Screening was carried out by varying the methanol/oil molar ratio and temperature (Table 2).

The results show the crucial role of temperature with a decrease in yields by lowering the temperature from 180 to 120 °C (Entry 4 vs. 1 or Entry 8 vs. 5). Besides the beneficial effect on reaction rate, a higher reaction temperature reduces the viscosity of the oil and improves mass transfer between oil and methanol. The methanol/oil molar ratio is also a key factor, as a larger excess of methanol favorably affects the conversion: a 20/1 methanol/oil molar ratio is enough to bring the conversion close to 100% at 160

°C (Entry 7). This result significantly improves the data obtained previously with the analogous complex derived from salen, demonstrating the validity of the structural motif choice as well as the importance of catalyst selection and process optimization. The robustness of the catalytic system was further verified against a severely acidified sunflower oil (AV 5.1 mg(KOH)/g(oil) due to the addition of oleic acid) using conditions reported in Table 2, Entry 9. As anticipated, biodiesel yield remained high at 85% ± 2%, accompanied by a simultaneous reduction in free acidity from 5.1 mg(KOH)/g(oil) to 3.0 mg(KOH)/g(oil).

Table 2. Biodiesel yields ^a using the **2H-OAc** catalyst on a waste sunflower oil ^b.

Entry	mol(MeOH)/mol(oil)	T, °C	Yield, %
1	10/1	120	80 ± 2
2	10/1	140	84 ± 2
3	10/1	160	87 ± 2
3' ^c	10/1	160	86 ± 2
4	10/1	180	91 ± 2
5	20/1	120	83 ± 2
6	20/1	140	88 ± 2
7	20/1	160	98 ± 2
8	20/1	180	97 ± 2
9 ^d	20/1	160	85 ± 2

^a t = 2 h; mol(Fe)/mol(oil) = 0.001/1. ^b AV = 0.34 mg(KOH)/g(oil); peroxide value = 16.8 meq(O₂)/kg(oil); iodine value: 126 g(I₂)/100 g(oil). ^c Fresh sunflower oil: AV = 0.1 mg(KOH)/g(oil); peroxide value = 1.95 meq(O₂)/kg(oil); iodine value: 129 g(I₂)/100 g(oil). Sunflower oil fatty acid composition: SFAs 8%_{mol}, MUFAs 41%_{mol}, PUFAs 51%_{mol}. ^d Acidified sunflower oil AV = 5.1 mg(KOH)/g(oil).

To validate the reliability of the catalyst, a test was conducted with the same waste sunflower and ethanol under previously optimized conditions (**2H-OAc** 0.1%_{mol}, 2 h, 160 °C, 20/1 mol(EtOH)/mol(oil)). The performance was confirmed to be satisfactory, achieving a yield of 76 ± 2%, with reduced activity (compared to methanol) in line with expectations due to the increase in the alkyl chain length [32].

Table 3 presents a comparison with some homogeneous and heterogeneous catalysts, both Brønsted acids or bases and Lewis acids. It emerges that temperatures and molar ratios, in some cases less favorable than those applied when KOH or specific heterogeneous catalytic systems are used, are largely compensated for by the low catalyst loading and its synthetic convenience. In fact, when dealing with waste cooking oil (WCO), a preliminary esterification step is necessary before using KOH (usually involving strong Brønsted acids), and many heterogeneous catalysts require very high loadings that are unlikely to be scalable. Moreover, in the case of heterogeneous catalysts, leaching investigations are rarely reported, making their performances difficult to assess and compare with our results. However, beyond these general considerations, for readers interested in a deeper analysis, some extensive reviews were recently published on this topic [33–36].

Table 3. Comparison with homogeneous and heterogeneous catalysts for biodiesel production.

Entry	Feedstock	Catalyst (Loading)	MR	ROH	T, °C	Time, min	Yield, %	Ref
1	POS	KOH (1.5%wt)	20/1	MeOH	60	60	93	[37]
2	SFO/SBO	H ₂ SO ₄ (2.5%wt)	6/1	MeOH	60	60	96	[38]
3	WCO	Zn(OAc) ₂ /SiO ₂ (3%wt)	30/1	MeOH	140	120	88	[39]
4	JJO	(C ₄ H ₉) ₂ Sn(OOCCH ₃) ₂ (1%wt)	23/1	MeOH	60	60	93	[40]
5	SBO	NaOH (0.3%wt)	12/1	EtOH	70	60	97	[41]
6	MIO	H ₂ SO ₄ (6%wt)	9/1	EtOH	78	300	92	[42]

Table 3. Cont.

Entry	Feedstock	Catalyst (Loading)	MR	ROH	T, °C	Time, min	Yield, %	Ref
7	MAL	WO ₃ /ZrO ₂ (15%wt)	12/1	MeOH	100	180	95	[43]
8	SFO	CaO—700 °C activated (1%wt)	13/1	MeOH	60	100	94	[44]
9	SFO	MgO/MgFe ₂ O ₄ (4%wt)	12/1	MeOH	110	240	91	[45]
10	SBPO	Fe ₃ O ₄ -ZIF-8- H ₆ PV ₃ MoW ₈ O ₄₀ (6%wt)	30/1	MeOH	160	600	93	[46]
11	MAL	CaO(0.6wt)/Al ₂ O ₃ (0.4wt) (12%wt)	48/1	EtOH	50	120	99	[47]
12	SBO	SO ₄ /ZrO ₂ (5%wt)	20/1	EtOH	120	60	92	[48]
13	WFO	5 Novozyme 435 (50%wt)	35/1	EtOH	35	480	83	[49]

Feedstock abbreviations: Palm Oil Sludge, POS; Sunflower oil, SFO; Soybean oil, SBO; Waste cooking oil, WCO; Jojoba oil, JJO; Microalgal lipids, MAL; Waste fish oil, WFO; Madhuca indica oil, MIO. MR: mol(ROH)/mol(oil) molar ratio.

A curve expressing the conversion over time was also determined for Entry 7 of Table 2, by collecting data every 15 min/30 min over a range of 120 min. The results are graphically shown in Figure 5.

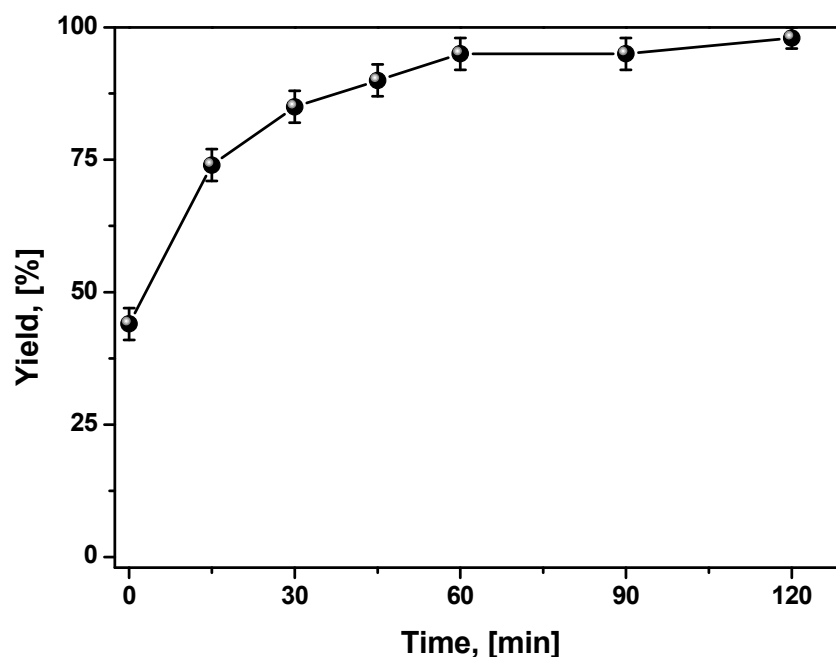
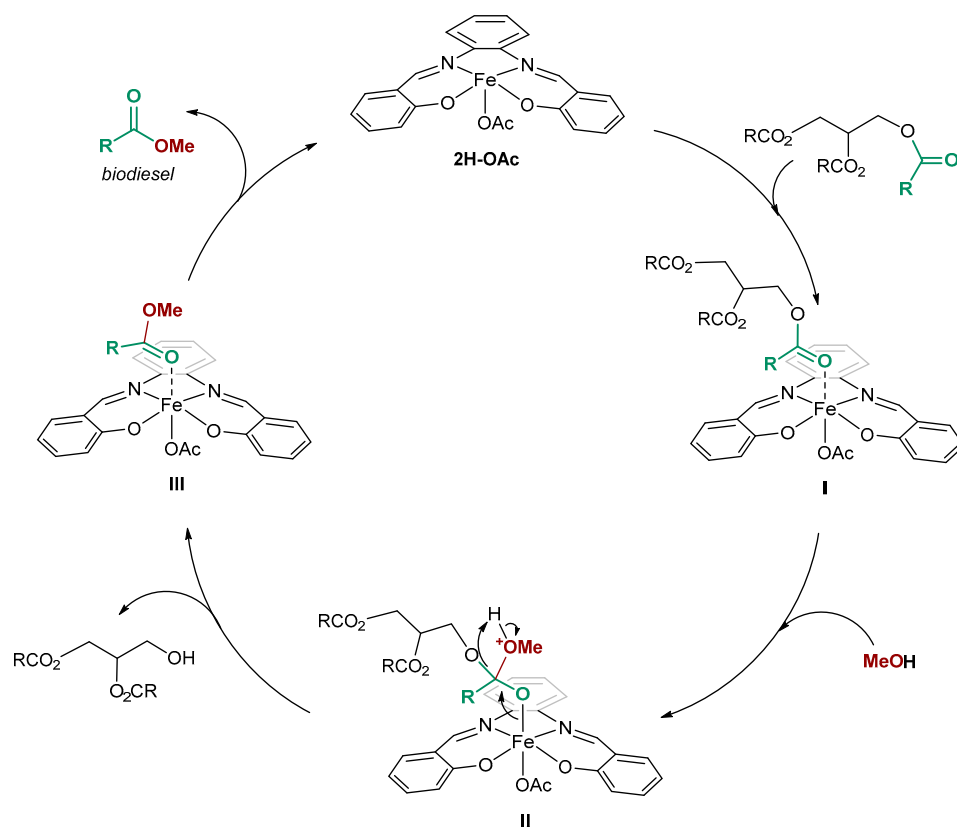


Figure 5. Formation of biodiesel according to Entry 7 of Table 2.

The plausible key steps of the reaction mechanism are illustrated in Scheme 4. The carbonyl group of the triglyceride is activated upon coordination to the iron(III) ion (in I). The nucleophilic attack of methanol yields tetrahedral intermediate II which undergoes an intramolecular rearrangement leading to the release of biodiesel, diglyceride and III. It is reasonable to hypothesize the same mechanism in the case where the alcohol is ethanol, and the slight decrease in conversion is attributed to its larger steric hindrance, leading to reduced accessibility to the catalytic site.



Scheme 4. Proposed key steps for transesterification.

3. Materials and Methods

Iron(III) chloride hexahydrate, anhydrous iron(II) acetate, 1,2-phenylenediamine, 4-nitro-*o*-phenylenediamine, salicylaldehyde, 5-methylsalicylaldehyde, 5-methoxysalicylaldehyde and the solvents were purchased from Merck KGaA, (Darmstadt, Germany) and used as received. Catalysts **2H-OAc**, **2H-Cl** and **2Ome-Cl** [26–28] and ligand **L-Me** [50] were described in the literature. Methodologies are briefly reported in Section 3.1. NMR spectra were recorded with a Bruker Avance Ultrashield 400 (Bruker Corporation, Billerica, MA, USA) at a proton frequency of 400 MHz or with a Varian 500 Oxford (Varian Inc., Palo Alto, CA, USA) at a proton frequency of 500 MHz. The following abbreviations are used for NMR multiplicities: s, singlet; d, doublet; dd, doublet of doublets; t, triplet; td, triplet of doublets; m, multiplet; app, apparent. Matrix-assisted laser desorption/ionization (MALDI) mass spectrometry (MS) experiments were performed on a 5800 MALDI-TOF-TOF AB SCIEX (SCIEX, Toronto, Canada) equipped with a nitrogen laser (337 nm). IR spectra were recorded on a JASCO FT/IR-430 spectrophotometer (JASCO EUROPE, Cremella, Italy). Melting points were measured with a Digital Melting Point Apparatus Electrothermal IA9000 Series (Electrothermal Ltd., London, UK). The following abbreviations are used for FT-IR signals: s, strong; m, medium; w, weak; br, broad; sat, saturated. Catalysis was performed in a Low-Pressure Pari[®] Reactor model 5100 equipped with an MI-heating band purchased from Watlow Italy s.r.l. (Corsico, Italy).

3.1. Vegetable Oil Characterizations

Acidity value (AV, or Free Fatty Acids content, FFAs), peroxide value (PV), and iodine value (IV) were determined following European regulations (EU) 2568/91 and 2016/1227—Annex 2 (determination of free fatty acids, cold method) [51,52]. For all the titration procedures, three determinations and a blank test were performed. The methods are briefly reported in supporting information (Paragraph S1).

3.2. Synthesis of L-NO₂

To a suspension of 4-nitro-*o*-phenylenediamine (1.53 g, 10.0 mmol) in toluene (25 mL) salicylaldehyde was added dropwise (14.7 g, 120 mmol). The resulting mixture was heated at reflux for 20 h. A yellow precipitate appeared after cooling the mixture at room temperature. The precipitate was filtered, washed thoroughly with toluene and hexane and dried under vacuum to obtain 2.78 g of the ligand. Yield: 70%. ¹H NMR (CDCl₃, 500 MHz, 298 K): δ 12.54 (s, 1H), 12.47 (s, 1H), 8.73 (s, 1H), 8.65 (s, 1H), 8.23 (dd, 1H, ³J_{H-H} = 8.55 Hz, ⁴J_{H-H} = 2.49 Hz), 8.15 (d, 1H, ⁴J_{H-H} = 2.49 Hz), 7.46–7.40 (m, 4H), 7.33 (d, 1H, ³J_{H-H} = 8.48 Hz), 7.06 (app t, 2H, ³J_{H-H} = 7.24 Hz), 6.97 (td, 1H, ³J_{H-H} = 7.41 Hz, ⁴J_{H-H} = 1.06 Hz), 6.96 (dt, 1H, ³J_{H-H} = 7.50 Hz, ⁴J_{H-H} = 1.07 Hz).

3.3. Synthesis of 2Me-OAc, 2OMe-OAc and 2'H-OAc

Iron(II) acetate (0.174 g, 1.00 mmol) was suspended in 10 mL of ethanol. The appropriate salophen ligand (1.00 mmol) was added as a solid to this mixture, which was refluxed for 2.5 h. After cooling at room temperature, the filtered product was washed with cold ethanol (3 × 10 mL), and dried. Yield: 75–85%. **2Me-OAc**: IR (cm⁻¹): 1617 (m, C=N), 1465 (s, C=O, acetate, covered by nujol), MALDI (TOF-TOF) *m/z* for [M-OAc]⁺: calculated for [FeC₂₂H₁₈N₂O₂⁺], 398.07, found, 397.85; **2OMe-OAc**: IR (cm⁻¹): 1617 (m, C=N), 1465 (s, C=O, acetate, covered by nujol), MALDI (TOF-TOF) *m/z* for [M-OAc]⁺: calculated for [FeC₂₂H₁₈N₂O₄⁺], 430.06, found, 429.83; **2'H-OAc**: IR (cm⁻¹): 1608 (s, C=N), 1465 (s, C=O, acetate, covered by nujol) 1575 (m), 1343 (w) (NO₂, nitro), MALDI (TOF-TOF) *m/z* for [M-OAc]⁺: calculated for [FeC₂₀H₁₃N₃O₄⁺], 415.03, found, 414.81.

3.4. Synthesis of 2Me-Cl

Ligand **L-Me** (0.120 g 0.350 mmol) was dissolved under stirring in 10 mL of dichloromethane at room temperature in a round-bottom flask. Iron(III) chloride hexahydrate (0.097 g, 0.36 mmol) was subsequently added to the mixture. The bright yellow suspension immediately turned dark brown. The reaction mixture was left stirring for 1 h. A solution of triethylamine (98 μL, 0.702 mmol) in 2 mL of dichloromethane was added, and the dark reddish-brown mixture was refluxed. After 2 h, stirring and heating were suspended, and the solution was extracted with water (3 × 30 mL) to remove triethylammonium chloride and excess iron(III) chloride. The organic phase was then recovered, and the solvent was slowly removed under vacuum. Dark brown powder was obtained that was washed with cold methanol (3 × 10 mL) and dried under vacuum. Yield: 75%. IR (cm⁻¹): 1617 (m, C=N), MALDI (TOF-TOF) *m/z* for [M-Cl]⁺: calculated for [FeC₂₂H₁₈N₂O₂⁺], 398.07, found, 397.85.

3.5. Synthesis of 2''H-OAc

A dried glass reaction pressure tube equipped with a magnetic stir bar was charged with **2'H-OAc** (0.474 g, 1.00 mmol), bis(pinacolato)diboron (0.787 g, 3.10 mmol) and *t*-BuOK (0.135 g, 1.20 mmol) and *i*-propanol (4.0 mL), and the mixture was then stirred at 110 °C for 1 day. After cooling at room temperature, the crude product was diluted with water and then washed with water (3 × 5 mL), cold ethanol (2 × 5 mL) and dried under vacuum. Yield: 80–83%. IR (cm⁻¹): 3347 (w, NH₂, amine), 1609 (s, C=N), 1465 (s, C=O, acetate, covered by nujol), MALDI (TOF-TOF) *m/z* for [M-OAc]⁺: calculated for [FeC₂₀H₁₅N₃O₂⁺], 385.05, found, 384.84.

3.6. Catalytic Runs

Catalytic tests were carried out by introducing the corresponding amount of vegetable (fresh or waste) oil, methanol and iron catalyst (0.1% molar loading) into a stainless steel Parr[®] batch reactor (Parr Instrument Company, Moline, IL, USA) equipped with a thermostatic heating band.

The temperature was raised to the correct value and kept for the appropriate time. At the end of the reaction, the heating band was turned off and removed. Then, the

vessel was rapidly cooled in an ice bath. The reaction mixture was evaporated under vacuum to remove excess methanol. The resulting oily fraction was analyzed via ^1H NMR spectroscopy to determine the yield of the reaction. Relevant signals for the quantification of the reaction yield were:

- the singlet at δ 3.7 (b), related to the methoxyl group in the product;
- the triplet at δ 2.3 (d), attributed to the methylene protons in α position to the carbonyl group, present both in the reagent and the product.

The yield is obtained with the following Formula (1), in which the ratio b/d is normalized by the number of protons related to each signal (^1H NMR example in Figure 6):

$$\text{Yield}(\%) = 100 \times \frac{\int b/3}{\int d/2} \quad (1)$$

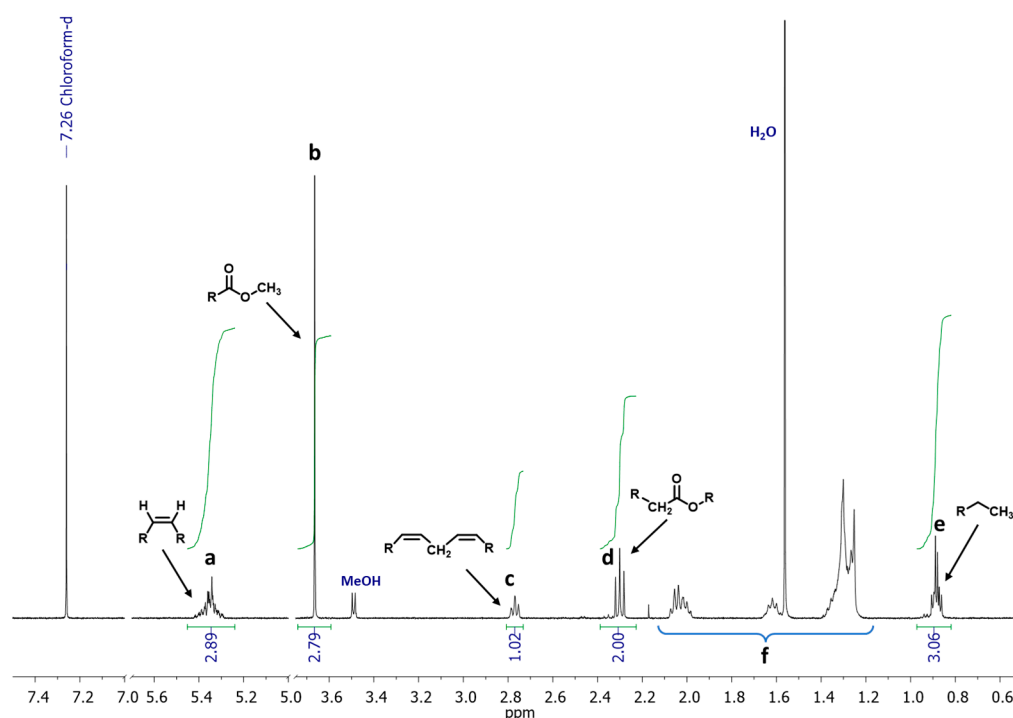


Figure 6. ^1H NMR spectrum in CDCl_3 at 298 K at 400 MHz of biodiesel produced from waste sunflower oil according to Entry 2 of Table 2. ($T = 160\text{ }^\circ\text{C}$; $t = 2\text{ h}$; $\text{mol}(\text{Fe})/\text{mol}(\text{oil}) = 0.001/1$; $\text{mol}(\text{MeOH})/\text{mol}(\text{oil}) = 10/1$). Protons “f” are related to aliphatic chains.

4. Conclusions

This work demonstrates the great potential of homogeneous catalysis also in the emerging field of biomass transformation to obtain bioproducts and biofuels. Indeed, the selection of a panel of iron(III) complexes containing salophen ligands allowed the evaluation of their performance in the production of biodiesel from vegetable oils. The versatility of the salophen ligand’s structure has enabled discrimination between subtle electronic properties and the making of hypotheses about the factors that modulate the catalytic activity of the complexes. In all cases, they proved to be active even at very low loadings (down to 0.1% mol/mol vs. oil), and under these conditions, it was possible to select the most promising one for catalyzing the reaction of an authentic exhausted matrix. The results validated this choice, as its complete conversion to biodiesel was obtained under favorable conditions. The price of the catalyst is surely higher compared to that of simple Brønsted acids or bases (e.g., H_2SO_4 , KOH), but still reasonable given the widespread availability of ingredients, whose value would certainly be reduced in the case of bulk purchases. To this evaluation, the one related to the simplification of manufacturing compared to that with strong Brønsted acids/bases should be added,

contributing to a significant economic advantage (e.g., limited washings, no feed pre-treatment, the possibility of using less corrosion-resistant equipment).

These findings emphasize the importance of catalyst selection and process optimization, open the door to more sustainable and efficient biodiesel production methods and hold significant implications for the utilization of waste cooking oils as a valuable resource in the biofuel industry.

Supplementary Materials: The following supporting information can be downloaded at: <https://www.mdpi.com/article/10.3390/catal13121496/s1>, Figure S1: FT-IR spectrum, in nujol, of complex **2Me-OAc**; Figure S2: FT-IR spectrum, in nujol, of complex **2OMe-OAc**; Figure S3: FT-IR spectrum, in nujol, of complex **2'H-OAc**; Figure S4: FT-IR spectrum, in nujol, of complex **2Me-Cl**; Figure S5: FT-IR spectrum, in nujol, of complex **2''H-OAc**; Table S1: Melting points (decomposition) of the catalysts; Paragraph S1: Vegetable oil characterization methods.

Author Contributions: Conceptualization, R.E. and F.R.; methodology, V.L., M.M., M.E.C. and G.P.; validation, M.E.C., R.E. and F.R.; formal analysis, V.L. and D.G.; investigation, V.L., M.M. and D.G.; data curation, M.E.C., R.E. and F.R.; writing—original draft preparation, M.M. and F.R.; writing—review and editing, all authors; supervision, R.E. and F.R.; project administration, F.R.; funding acquisition, F.R. All authors have read and agreed to the published version of the manuscript.

Funding: This study was carried out within the Agritech National Research Center and received funding from the European Union Next-GenerationEU (PIANO NAZIONALE DI RIPRESA E RESILIENZA (PNRR) MISSIONE 4 COMPONENTE 2, INVESTIMENTO 1.4-D.D. 1032 17/06/2022, CN00000022). This manuscript reflects only the authors' views and opinions, neither the European Union nor the European Commission can be considered responsible for them.

Data Availability Statement: The data presented in this study are available in the article and supplementary material.

Conflicts of Interest: The authors declare no conflict of interest.

References

1. Maity, S.K. Opportunities, recent trends and challenges of integrated biorefinery: Part I. *Renew. Sustain. Energy Rev.* **2015**, *43*, 1427–1445. [[CrossRef](#)]
2. Moncada, J.; Tamayo, J.A.; Cardona, C.A. Integrating first, second, and third generation biorefineries: Incorporating microalgae into the sugarcane biorefinery. *Chem. Eng. Sci.* **2014**, *118*, 126–140. [[CrossRef](#)]
3. Anastas, P.; Eghbali, N. Green Chemistry: Principles and Practice. *Chem. Soc. Rev.* **2010**, *39*, 301–312. [[CrossRef](#)]
4. Xu, H.; Ou, L.; Li, Y.; Hawkins, T.R.; Wang, M. Life Cycle Greenhouse Gas Emissions of Biodiesel and Renewable Diesel Production in the United States. *Environ. Sci. Technol.* **2022**, *56*, 7512–7521. [[CrossRef](#)]
5. Park, S.H.; Khan, N.; Lee, S.; Zimmermann, K.; DeRosa, M.; Hamilton, L.; Hudson, W.; Hyder, S.; Serratos, M.; Sheffield, E.; et al. Biodiesel Production from Locally Sourced Restaurant Waste Cooking Oil and Grease: Synthesis, Characterization, and Performance Evaluation. *ACS Omega* **2019**, *4*, 7775–7784. [[CrossRef](#)]
6. Mattos, R.A.d.; Bastos, F.A.; Tubino, M. Correlation Between the Composition and Flash Point of Diesel-Biodiesel Blends. *J. Braz. Chem. Soc.* **2015**, *26*, 393–395. [[CrossRef](#)]
7. Tan, H.W.; Abdul Aziz, A.R.; Aroua, M.K. Glycerol production and its applications as a raw material: A review. *Renew. Sustain. Energy Rev.* **2013**, *27*, 118–127. [[CrossRef](#)]
8. Fonseca, J.M.; Teleken, J.G.; de Cinque Almeida, V.; da Silva, C. Biodiesel from waste frying oils: Methods of production and purification. *Energy Convers. Manag.* **2019**, *184*, 205–218. [[CrossRef](#)]
9. Khodadadi, M.R.; Malpartida, I.; Tsang, C.-W.; Lin, C.S.K.; Len, C. Recent advances on the catalytic conversion of waste cooking oil. *Mol. Catal.* **2020**, *494*, 111128. [[CrossRef](#)]
10. Consorzio Nazionale di Raccolta e Trattamento Degli oli e Dei Grassi Vegetali ed Animali Esausti. Available online: <https://www.conoe.it/> (accessed on 11 October 2023).
11. Wang, B.; Wang, B.; Shukla, S.K.; Wang, R. Enabling Catalysts for Biodiesel Production via Transesterification. *Catalysts* **2023**, *13*, 740. [[CrossRef](#)]
12. Zeng, D.; Yang, L.; Fang, T. Process optimization, kinetic and thermodynamic studies on biodiesel production by supercritical methanol transesterification with CH₃ONa catalyst. *Fuel* **2017**, *203*, 739–748. [[CrossRef](#)]
13. Jalkh, R.; El-Rassy, H.; Chehab, G.R.; Abiad, M.G. Assessment of the Physico-Chemical Properties of Waste Cooking Oil and Spent Coffee Grounds Oil for Potential Use as Asphalt Binder Rejuvenators. *Waste Biomass Valorization* **2018**, *9*, 2125–2132. [[CrossRef](#)]
14. Benessere, V.; Cucciolo, M.E.; Esposito, R.; Lega, M.; Turco, R.; Ruffo, F.; Di Serio, M. A novel and robust homogeneous supported catalyst for biodiesel production. *Fuel* **2016**, *171*, 1–4. [[CrossRef](#)]

15. Benessere, V.; Cucciolito, M.E.; Poggetto, G.D.; Di Serio, M.; Granados, M.L.; Ruffo, F.; Vitagliano, A.; Vitiello, R. Strategies for immobilizing homogeneous zinc catalysts in biodiesel production. *Catal. Commun.* **2014**, *56*, 81. [[CrossRef](#)]
16. Esposito, R.; Melchiorre, M.; Annunziata, A.; Cucciolito, M.E.; Ruffo, F. Emerging catalysis in biomass valorisation: Simple Zn(II) catalysts for fatty acids esterification and transesterification. *ChemCatChem* **2020**, *12*, 5858–5879. [[CrossRef](#)]
17. Di Serio, M.; Carotenuto, G.; Cucciolito, M.E.; Lega, M.; Ruffo, F.; Tesser, R.; Trifuoggi, M. Schiff base complexes of zinc(II) as catalysts for biodiesel production. *J. Mol. Catal. A Chem.* **2012**, *353–354*, 106–110. [[CrossRef](#)]
18. Ferreira, A.B.; Lemos Cardoso, A.; da Silva, M.J. Tin-Catalyzed Esterification and Transesterification Reactions: A Review. *ISRN Renew. Energy* **2012**, *2012*, 142857. [[CrossRef](#)]
19. Zubair, M.; Sirajuddin, M.; Haider, A.; Hussain, I.; Tahir, M.N.; Ali, S. Organotin (IV) Complexes as Catalyst for Biodiesel Formation: Synthesis, Structural Elucidation and Computational Studies. *Appl. Organomet. Chem.* **2020**, *34*, e5305. [[CrossRef](#)]
20. Melchiorre, M.; Amoresano, A.; Budzelaar, P.H.M.; Cucciolito, M.E.; Mocerino, F.; Pinto, G.; Ruffo, F.; Tuzi, A.; Esposito, R. Parts-Per-Million (Salen)Fe(III) Homogeneous Catalysts for the Production of Biodiesel from Waste Cooking Oils. *Catal. Lett.* **2022**, *152*, 3785–3794. [[CrossRef](#)]
21. Vasić, K.; Hojnik Podrepšek, G.; Knez, Ž.; Leitgeb, M. Biodiesel Production Using Solid Acid Catalysts Based on Metal Oxides. *Catalysts* **2020**, *10*, 237. [[CrossRef](#)]
22. Roy, T.; Sahani, S.; Madhu, D.; Chandra Sharma, Y. A clean approach of biodiesel production from waste cooking oil by using single phase BaSnO₃ as solid base catalyst: Mechanism, kinetics & E-study. *J. Clean. Prod.* **2020**, *265*, 121440. [[CrossRef](#)]
23. Dhawane, S.H.; Al-Sakkari, E.G.; Halder, G. Kinetic Modelling of Heterogeneous Methanolysis Catalysed by Iron Induced on Microporous Carbon Supported Catalyst. *Catal. Lett.* **2019**, *149*, 3508–3524. [[CrossRef](#)]
24. Olubunmi, B.E.; Karmakar, B.; Aderemi, O.M.; Auta, M.; Halder, G. Parametric optimization by Taguchi L9 approach towards biodiesel production from restaurant waste oil using Fe-supported anthill catalyst. *J. Environ. Chem. Eng.* **2020**, *8*, 104288. [[CrossRef](#)]
25. Taddeo, F.; Vitiello, R.; Tesser, R.; Melchiorre, M.; Eränen, K.; Salmi, T.; Russo, V.; Di Serio, M. Nonanoic acid esterification with 2-ethylhexanol: From batch to continuous operation. *Chem. Eng. J.* **2022**, *444*, 136572. [[CrossRef](#)]
26. Driscoll, O.J.; Hafford-Tear, C.H.; McKeown, P.; Stewart, J.A.; Kociok-Köhn, G.; Mahon, M.F.; Jones, M.D. The synthesis, characterisation and application of iron(iii)-acetate complexes for cyclic carbonate formation and the polymerisation of lactide. *Dalton Trans.* **2019**, *48*, 15049–15058. [[CrossRef](#)]
27. Gerloch, M.; Lewis, J.; Mabbs, F.E.; Richards, A. The preparation and magnetic properties of some Schiff base-iron(III) halide complexes. *J. Chem. Soc. A Inorg. Phys. Theor.* **1968**, 112–116. [[CrossRef](#)]
28. Hille, A.; Gust, R. Influence of methoxy groups on the antiproliferative effects of [FeIII(salophene-OMe)Cl] complexes. *Eur. J. Med. Chem.* **2010**, *45*, 5486–5492. [[CrossRef](#)]
29. Sakthivel, R.V.; Sankudevan, P.; Vennila, P.; Venkatesh, G.; Kaya, S.; Serdaroglu, G. Experimental and theoretical analysis of molecular structure, vibrational spectra and biological properties of the new Co(II), Ni(II) and Cu(II) Schiff base metal complexes. *J. Mol. Struct.* **2021**, *1233*, 130097. [[CrossRef](#)]
30. Lu, H.; Geng, Z.; Li, J.; Zou, D.; Wu, Y.; Wu, Y. Metal-Free Reduction of Aromatic Nitro Compounds to Aromatic Amines with B₂pin₂ in Isopropanol. *Org. Lett.* **2016**, *18*, 2774–2776. [[CrossRef](#)]
31. Tomita, K.; Ida, H. Studies on the formation of poly(ethylene terephthalate): 3. Catalytic activity of metal compounds in transesterification of dimethyl terephthalate with ethylene glycol. *Polymer* **1975**, *16*, 185–190. [[CrossRef](#)]
32. Likozar, B.; Levec, J. Transesterification of canola, palm, peanut, soybean and sunflower oil with methanol, ethanol, isopropanol, butanol and tert-butanol to biodiesel: Modelling of chemical equilibrium, reaction kinetics and mass transfer based on fatty acid composition. *Appl. Energy* **2014**, *123*, 108–120. [[CrossRef](#)]
33. Bashir, M.A.; Wu, S.; Zhu, J.; Krosuri, A.; Khan, M.U.; Ndeddy Aka, R.J. Recent development of advanced processing technologies for biodiesel production: A critical review. *Fuel Process. Technol.* **2022**, *227*, 107120. [[CrossRef](#)]
34. Singh, D.; Sharma, D.; Soni, S.L.; Sharma, S.; Kumar Sharma, P.; Jhalani, A. A review on feedstocks, production processes, and yield for different generations of biodiesel. *Fuel* **2020**, *262*, 116553. [[CrossRef](#)]
35. Mahlia, T.M.I.; Syazmi, Z.A.H.S.; Mofijur, M.; Abas, A.E.P.; Bilad, M.R.; Ong, H.C.; Silitonga, A.S. Patent landscape review on biodiesel production: Technology updates. *Renew. Sustain. Energy Rev.* **2020**, *118*, 109526. [[CrossRef](#)]
36. Stamenković, O.S.; Veličković, A.V.; Veljković, V.B. The production of biodiesel from vegetable oils by ethanolysis: Current state and perspectives. *Fuel* **2011**, *90*, 3141–3155. [[CrossRef](#)]
37. Abdullah; Rahmawati Sianipar, R.N.; Ariyani, D.; Nata, I.F. Conversion of palm oil sludge to biodiesel using alum and KOH as catalysts. *Sustain. Environ. Res.* **2017**, *27*, 291–295. [[CrossRef](#)]
38. Farag, H.A.; El-Maghraby, A.; Taha, N.A. Optimization of factors affecting esterification of mixed oil with high percentage of free fatty acid. *Fuel Process. Technol.* **2011**, *92*, 507–510. [[CrossRef](#)]
39. Corro, G.; Bañuelos, F.; Vidal, E.; Cebada, S. Measurements of surface acidity of solid catalysts for free fatty acids esterification in *Jatropha curcas* crude oil for biodiesel production. *Fuel* **2014**, *115*, 625–628. [[CrossRef](#)]
40. Shah, M.; Ali, S.; Tariq, M.; Khalid, N.; Ahmad, F.; Khan, M.A. Catalytic conversion of jojoba oil into biodiesel by organotin catalysts, spectroscopic and chromatographic characterization. *Fuel* **2014**, *118*, 392–397. [[CrossRef](#)]
41. Kucek, K.T.; César-Oliveira, M.A.F.; Wilhelm, H.M.; Ramos, L.P. Ethanolysis of Refined Soybean Oil Assisted by Sodium and Potassium Hydroxides. *J. Am. Oil Chem. Soc.* **2007**, *84*, 385–392. [[CrossRef](#)]

42. Saravanan, N.; Puhan, S.; Nagarajan, G.; Vedaraman, N. An experimental comparison of transesterification process with different alcohols using acid catalysts. *Biomass Bioenergy* **2010**, *34*, 999–1005. [CrossRef]
43. Guldhe, A.; Singh, P.; Ansari, F.A.; Singh, B.; Bux, F. Biodiesel synthesis from microalgal lipids using tungstated zirconia as a heterogeneous acid catalyst and its comparison with homogeneous acid and enzyme catalysts. *Fuel* **2017**, *187*, 180–188. [CrossRef]
44. Granados, M.L.; Poves, M.D.Z.; Alonso, D.M.; Mariscal, R.; Galisteo, F.C.; Moreno-Tost, R.; Santamaria, J.; Fierro, J.L.G. Biodiesel from sunflower oil by using activated calcium oxide. *Appl. Catal. B Environ.* **2007**, *73*, 317–326. [CrossRef]
45. Alaei, S.; Haghighi, M.; Toghiani, J.; Rahmani Vahid, B. Magnetic and reusable MgO/MgFe₂O₄ nanocatalyst for biodiesel production from sunflower oil: Influence of fuel ratio in combustion synthesis on catalytic properties and performance. *Ind. Crops Prod.* **2018**, *117*, 322–332. [CrossRef]
46. Xie, W.; Gao, C.; Li, J. Sustainable biodiesel production from low-quantity oils utilizing H₆PV₃MoW₈O₄₀ supported on magnetic Fe₃O₄/ZIF-8 composites. *Renew. Energy* **2021**, *168*, 927–937. [CrossRef]
47. Turkkul, B.; Deliismail, O.; Seker, E. Ethyl esters biodiesel production from *Spirulina* sp. and *Nannochloropsis oculata* microalgal lipids over alumina-calcium oxide catalyst. *Renew. Energy* **2020**, *145*, 1014–1019. [CrossRef]
48. Garcia, C.M.; Teixeira, S.; Marciniuk, L.L.; Schuchardt, U. Transesterification of soybean oil catalyzed by sulfated zirconia. *Bioresour. Technol.* **2008**, *99*, 6608–6613. [CrossRef]
49. Marín-Suárez, M.; Méndez-Mateos, D.; Guadix, A.; Guadix, E.M. Reuse of immobilized lipases in the transesterification of waste fish oil for the production of biodiesel. *Renew. Energy* **2019**, *140*, 1–8. [CrossRef]
50. Das, T.K.; Ghosh, A.; Balanna, K.; Behera, P.; Gonnade, R.G.; Marelli, U.K.; Das, A.K.; Biju, A.T. N-Heterocyclic Carbene-Catalyzed Umpolung of Imines for the Enantioselective Synthesis of Dihydroquinoxalines. *ACS Catal.* **2019**, *9*, 4065–4071. [CrossRef]
51. Commission Implementing Regulation (EU) 2016/1227 of 27 July 2016 Amending Regulation (EEC) No 2568/91 on the Characteristics of Olive Oil and Olive-Residue Oil and on the Relevant Methods of Analysis. Available online: https://eur-lex.europa.eu/eli/reg_impl/2016/1227/oj (accessed on 11 October 2023).
52. Commission Regulation (EEC) No 2568/91 of 11 July 1991 on the Characteristics of Olive Oil and Olive-Residue Oil and on the Relevant Methods of Analysis. Available online: <https://eur-lex.europa.eu/eli/reg/1991/2568/oj/eng> (accessed on 11 October 2023).

Disclaimer/Publisher’s Note: The statements, opinions and data contained in all publications are solely those of the individual author(s) and contributor(s) and not of MDPI and/or the editor(s). MDPI and/or the editor(s) disclaim responsibility for any injury to people or property resulting from any ideas, methods, instructions or products referred to in the content.